

CHITOSAN NANOPARTICLE AS A DELIVERY SYSTEM FOR POLYPHENOLS FROM MENIRAN EXTRACT (*PHYLLANTHUS NIRURI* L.): FORMULATION, OPTIMIZATION, AND IMMUNOMODULATORY ACTIVITY

GALIH PRATIWI^{1,2}, RONNY MARTIEN^{2,*}, RETNO MURWANTI³

¹Department of Pharmacy, STIKES Aisyiyah Palembang, Sumatera Selatan, Indonesia, ²Department of Pharmaceutics, Faculty of Pharmacy, Universitas Gadjah Mada, Sleman, D. I. Yogyakarta, Indonesia, ³Department of Pharmacology and Clinical Pharmacy, Faculty of Pharmacy, Universitas Gadjah Mada, Sleman, D. I. Yogyakarta, Indonesia
Email: ronnymartien@ugm.ac.id

Received: 27 Sep 2018, Revised and Accepted: 09 Jan 2019

ABSTRACT

Objective: This study aims to formulate meniran extract into polymeric nanoparticles. Better stability of active substances in formulas compared to unformulated extracts is expected to increase immunomodulatory activity.

Methods: Nanoparticles were formulated using ionic gelation method with chitosan and tripolyphosphate polymers. Optimize the mixture of nanoparticles using simplex lattice design (SLD) with the help of Design-Expert (DX) software. Evaluation of particle size and potential zeta using dynamic light scattering (DLS). Interactions between components were analyzed using Fourier transform infrared spectrophotometry-attenuated total reflectance (FTIR-ATR) and morphology of the lyophilization results observed using scanning electron microscopy (SEM). Immunomodulatory tests using the latex assay method. The parameters tested included phagocytosis index, phagocytic activity, and nitric oxide secretion.

Results: The optimum mixture of the formulation process was obtained in the composition of chitosan 0.270 %, extract 0.626 %, and tripolyphosphate 0.074 % with desirability value of 0.841. Optimal response with particle size 434.7±3.90 d. nm, polydispersity index 0.285±0.03 and entrapment efficiency 62.98±0.65 %. The zeta potential value in the optimum formula is 11.9±0.1 mV with a positive charge. Phagocytosis index and phagocytic activity of nanoparticles differed significantly ($p<0.05$) compared with unformulated extracts.

Conclusion: Meniran extract was successfully formulated into polymeric nanoparticles using chitosan-tripolyphosphate polymer. The developed nanoparticles have the immunomodulatory activity that is better than unformulated extract.

Keywords: *Phyllanthus niruri* L., polyphenols, Chitosan nanoparticles, Immunomodulatory, Phagocytosis

© 2019 The Authors. Published by Innovare Academic Sciences Pvt Ltd. This is an open-access article under the CC BY license (<http://creativecommons.org/licenses/by/4.0/>)
DOI: <http://dx.doi.org/10.22159/ijap.2019v11i2.29999>

INTRODUCTION

Phyllanthus niruri L. with the local name meniran (Indonesia) is one of the natural ingredients that have pharmacological activities. The herbal ingredients of this plant based on clinical trials have immunomodulatory activity [1]. The extract has been reported to increase specific and non-specific immune responses and is useful in immunodeficiency conditions [2, 3]. Meniran extract has been shown to increase macrophage phagocytic activity and nitric oxide production [4]. Many polyphenol compounds have been reported to have positive pharmacological effects [5-7]. In this case, the primary compound responsible for increasing the immune system is polyphenols, especially flavonoids [8].

Oral administration is widely used in immunomodulatory therapy because of its comfort and superiority. However, poor solubility and risk of first pass metabolism cause problems in bioavailability so that the immunomodulatory effects are not optimal [9, 10]. The problem of instability and solubility of a drug molecule can be solved using biodegradable polymer nanoparticle technology [11]. Nanotechnology applications can be a solution for solubility, bioavailability and open new opportunities to develop nano-delivery systems for active ingredients based on natural materials [12, 13].

Drug delivery systems such as polymeric nanoparticles, microparticles, and emulsions have been applied to improve stability, protect bioactive components from metabolism and enzymatic degradation due to temperature or light [14]. One of the polymers that are widely used in drug delivery systems based on nanoparticles is chitosan [15]. Chitosan is biodegradable, biocompatible, and easily processed in various forms [16, 17]. Negatively charged tripolyphosphate compounds (TPP) are used in the formation of nanoparticles using positively charged chitosan. In the formulation, chitosan will be stabilized by TPP through intramolecular hydrogen bonds [18, 19].

Research results related to the development of polyphenol delivery systems from various plant extracts have been widely reported [20, 21]. However, as far as our search and knowledge, chitosan-TPP formulations to deliver meniran extracts and immunomodulatory assay have never been reported. This study aims to formulate chitosan, TPP, and meniran extract into polymeric nanoparticles using ionic gelation method. Characterization includes particle size diameter, polydispersity index, zeta potential, and entrapment efficiency. Profiling using Fourier Transform Infrared Spectrophotometry-Attenuated Total Reflectance (FTIR-ATR) and scanning electron microscopy (SEM). Immunomodulatory activity was evaluated from phagocytosis index, phagocytic activity, and nitric oxide secretion. Furthermore, it is expected to obtain nanoparticles-based meniran extract immunomodulatory product.

MATERIALS AND METHODS

Chemicals and sampels

Standard quercetin, chitosan, tripolyphosphate, and latex beads polystyrene were obtained from Sigma-Aldrich (St. Louis, MO, USA). Glacial acetic acid, giemsa, ethanol, and methanol were purchased from Merck (Darmstadt, Germany). Meniran (*Phyllanthus niruri* L.) were purchased from Merapi Farma (Sleman, Indonesia).

Preparation of chitosan nanoparticle loaded the meniran extract

Characterization of *Phyllanthus niruri* samples with specimen numbers of HS/PN/0003/17 stored in the Pharmacognosy Laboratory, Pharmaceutical Biology, STIKES Aisyiyah Palembang. Meniran extract (ME) was produced using the maceration method with 70 % ethanol solvent. Nanoparticle formulation uses ionic gelation method with modification [22,23]. Chitosan solution was obtained by dissolving chitosan powder in acetic acid (1 %, v/v). Nanoparticles were produced by mixing extract solution into

chitosan and adding TPP solution drop by drop. The nanoparticles formulated will then be abbreviated as meniran extract nanoparticles (ME-NPs).

Optimization design using simplex lattice design

Optimization in this formulation uses a design of experimental (DoE) approach. The design and processing of data using Design-Expert

software (Stat-Ease Inc., Minneapolis, MN, USA). The design chosen in DoE is part of the simplex lattice design (SLD) of mixture designs. The design uses independent variables chitosan (A; %), ME (B; %), and TPP (C; %). In the modeling, three responses were selected to be evaluated, namely particle size (Y_1), polydispersity index (Y_2), and entrapment efficiency (Y_3). The composition of the mixture of ingredients from each experiment is presented in table 1.

Table 1: Composition of mixtures in the simplex lattice design and experimental results

Run	A: Chitosan (%)	B: ME (%)	C: TPP (%)	Y_1^* : Particle size (d. nm)	Y_2^* : Polydispersity index (PDI)	Y_3^* : Entrapment efficiency (%)
1	0.270	0.680	0.020	530.9	0.464	50.95
2	0.360	0.590	0.020	679.8	0.507	52.84
3	0.360	0.590	0.020	691.5	0.513	52.02
4	0.315	0.590	0.065	485.1	0.329	61.23
5	0.270	0.635	0.065	391.9	0.261	62.61
6	0.285	0.650	0.035	552.2	0.341	54.89
7	0.285	0.605	0.080	435.0	0.268	64.06
8	0.330	0.605	0.035	632.3	0.359	53.48
9	0.270	0.590	0.110	704.2	0.424	68.77
10	0.300	0.620	0.050	573.4	0.428	57.63
11	0.315	0.635	0.020	642.1	0.442	52.52
12	0.270	0.680	0.020	539.0	0.467	51.45
13	0.315	0.635	0.020	770.3	0.393	52.83
14	0.270	0.590	0.110	729.3	0.381	67.42
15	0.315	0.590	0.065	465.2	0.421	61.92

*Data from each response is presented in mean ($n=3$)

Determination of particle size, zeta potential, and electrophoretic mobility

The particle size diameter, polydispersity index (PDI), zeta potential, and electrophoresis mobility were measured using a dynamic light scattering (DLS), namely Zetasizer Nano ZSP (Malvern Panalytical, UK). The data obtained as output from the Zetasizer 7.12 series software (Malvern Panalytical, UK). Measurements were adapted from previous studies with slight modifications [18, 24].

Determination of total flavonoid content (TFC)

Flavonoid content was determined using quercetin standard. Measurements by spectrophotometric method using aluminum chloride reagent with sufficient modification [25, 26]. Instrumentation used by Hitachi U-2900 (Hitachi, Japan) spectrophotometer.

Determination of entrapment efficiency (EE)

Nanoparticles were centrifuged at a speed of 15000 rpm at 24 °C for 30 min. The supernatant obtained was determined by TFC. Percentage of EE calculations using the formula:

$$\text{Entrapment efficiency (EE, \%)} = \frac{(\text{Total TFC in extract} - \text{Total TFC in the supernatant})}{\text{Total TFC in extract}} \times 100 \%$$

FTIR-ATR spectroscopy

The interaction between nanoparticle-making materials was observed qualitatively using FTIR-ATR. The analysis was carried out on ME-NPs optimum formula, chitosan, TPP, and ME. The Nicolet iS5 FTIR-ATR spectrometer equipped with Omnic (Thermo Scientific, USA) software was used in the functional group characterization. The analysis was carried out at 4000 to 500 cm^{-1} with a resolution of 4 cm^{-1} .

Morphology of prepared using SEM

ME-NPs solution was made in powder form (lyophilization). Morphology of the sample was observed using SEM with a JSM-6510 (Jeol, Tokyo, Japan).

Stability test of nanoparticles

The test was carried out by storing nanoparticles at a temperature of 25 to 30 °C for seven days. Nanoparticle samples measured particle diameter, PDI, zeta potential, and electrophoretic mobility on days 1, 3, and 7.

Experimental animals

The immunomodulatory assay using the latex assay method [4,9,27]. The animals used were Sprague Dawley rats with ethical clearance number 00150/04/IPPT/XII/2017. Experimental animals were adapted to the laboratory environment for one week. Rats grouping for immunomodulatory activity was done by dividing rats into five groups (water, CMC, ME, ME-NPs, and nanoparticles without extract (NPs-B)). Rats were treated according to their respective groups for seven days.

Macrophage isolation and culture

The peritoneal sheath was opened and cleaned using 70 % alcohol. Macrophage cells were taken with the help of RPMI-1640 medium in the peritoneal cavity. As much as 5 ml of macrophage fluid obtained was collected and put into a refrigerator. Macrophage liquid was centrifuged at 1200 rpm, 4 °C for 10 min. The supernatant was discarded, then 1 ml of complete RPMI was added to the pellet obtained. The amount obtained was calculated using a hemocytometer, then resuspended with a complete RPMI medium to obtain a cell suspension with a cell density of $2.5 \times 10^6/\text{ml}$.

The cell suspension was grown in microplate 24 wells with a volume of each well 200 μl ($5 \times 10^5/\text{ml}$) and given a slipcover. The cell suspension was incubated at 37 °C for 30 min in a 5 % CO_2 incubator. Furthermore, complete RPMI was added to 1 ml/well and incubated for 2 h. Subsequently, the media was discarded and added 1 ml complete RPMI/ well each time, incubated for 24 h in a 5 % CO_2 incubator and continued with activity test and phagocytosis index using the latex method *in vitro*.

Assay of macrophage phagocytosis

Non-specific phagocytosis assay was carried out using 20 μl latex beads (3 d. μm) suspended in 300 μl serum. The latex suspension is added to a well of 300 μl /well (5×10^6 latex), incubating for 60 min at 37°C. Then washing the suspension using PBS solution 2-3 times. Staining using giemsa 20 % with 30 min soaking. Calculation of the number of activated macrophages and the number of latex phagocytes in 100 macrophages. Every 100 cells of macrophages that phagocytize latex particles were calculated using a microscope. White latex and purple macrophages on observations using an inverted microscope (Zeiss, Olympus).

Determination of nitric oxide (NO)

The method of determining NO secretion using Griess reaction with slight modification. Samples were prepared after culturing for 24 h. A total of 100 μ l of samples and standard nitrite are included in the well. Furthermore, 100 μ l Griess solution (1 % sulfanilamide, 0.1 % naphthyl ethylenediamine in 5 % phosphoric acid) was added to each well-containing samples and standards. Microtiter plates were left at room temperature for 15 min until color changes occur. Absorbance measurements using a plate reader were carried out at a wavelength range of 520-590 nm. The levels of nitric oxide can be calculated by extrapolating data from standard curves using standard sodium nitrite.

Statistical analysis

Models in optimization were analyzed using Design-Expert software (Stat-Ease Inc., Minneapolis, MN, USA). All data are presented as means \pm SD. The statistical analysis of the experimental results was performed using the SPSS software (SPSS Inc, Chicago, IL, USA). A p -

value $<$ 0.05 was considered significant to compare immunomodulatory assay results.

RESULTS AND DISCUSSION

Optimization studies using the design of experiment (DoE) approach

Complete data on experimental results are presented in table 1. Data related to response results from 15 experiments scattered around the diagonal line on the normal plot of residuals (fig. 1-A, 1-B, and 1-C). This result indicates that the data is normally distributed and meets the requirements for the analysis of variance (ANOVA) test. Based on statistical analysis, the equation models of the three responses (Y_1 , Y_2 , and Y_3) can be used to predict the optimum mixture of the nanoparticle formulation process. Models of all three responses showed significant results ($p<$ 0.05) and the lack of fit was not significant ($p>$ 0.05). Particle size and polydispersity index as the first and second responses have quadratic models. The response of entrapment efficiency was obtained by a special quartic model.

Table 2: Analysis of variance from the equation model obtained

Parameter	Y_1 : Particle size (d. nm)	Y_2 : Polydispersity index (PDI)	Y_3 : Entrapment efficiency (%)
Standard deviation	48.27	0.0491	0.5955
Mean	588.15	0.3999	57.64
CV (%)	8.21	12.27	1.03
Press	50380.37	0.0452	38.33
Value R^2	0.8869	0.7412	0.9960
Adjusted R^2	0.8240	0.5974	0.9906
Predicted R^2	0.7283	0.4598	0.9275
Adequate precision	10.5377	7.3933	36.6193

Predicted vs. actual curves are used to detect values, or groups of values, that are not easily predicted by the model. The predictive and actual values of particle size are not much different (fig. 1-D, 1-E, 1-F) with the

difference in adjusted R^2 and predicted R^2 values less than 0.2 (table 2). These results indicate that there is no significant difference between the observed data and predictive data from the suggested model.

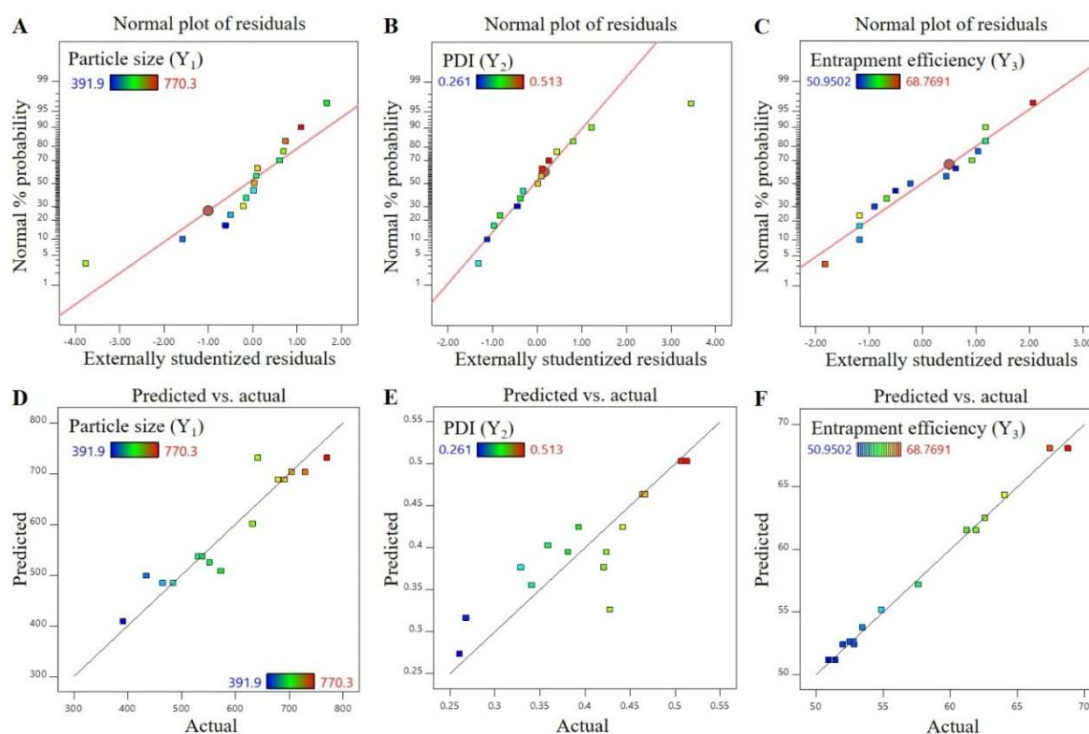


Fig. 1: Normal plot and predicted vs. actual plot

Based on the regression equation in table 3 shows a description of the influence of each material component as a factor in the response of the formed particle size. Each constituent

component of nanoparticles, namely chitosan (A), ME (B), and TPP (C) affects the increase in particle size, PDI, and EE produced.

Table 3: Type of model and equation of response

Response	Transform	Model	Equation
Y ₁ : Particle size	None	Quadratic	$Y_1 = 687.52A + 536.08B + 702.77C + 474.72AB - 843.31AC - 842.68BC$
Y ₂ : Polydispersity index	None	Quadratic	$Y_2 = 0.503A + 0.463B + 0.395C - 0.235AB - 0.290AC - 0.622BC$
Y ₃ : Entrapment efficiency	None	Special quartic	$Y_3 = 52.41A + 51.18B + 68.07C + 3.34AB + 5.15AC + 11.56BC - 188.61A^2BC - 28.02AB^2C + 4.31ABC^2$

Response of particle size (Y₁)

The interaction of chitosan-ME (AB) can increase the diameter of the particle size. The interaction of chitosan with TPP (AC) and ME interaction with TPP (BC) can reduce particle size. Chitosan as the main polymer will interact and bind the active compound from the extract in a certain amount so that the interaction of chitosan-ME (AB) will increase the particle size. TPP acts as a crosslinking agent,

in this case, its interaction with chitosan and extracts has a role in forming particles of a certain size [28,29]. Experiments at run 2, 3, 8, 9, 13, and 14 resulted in an average particle size diameter above 600 nm. Particle size that is too large is strongly influenced by the interaction of extracts and TPP. Experiments at run 5 and 12 proved that the same chitosan concentration (0.270%) gave different particle sizes at different ME (0.635% and 0.680%) and TPP (0.06% and 0.02%) concentrations.

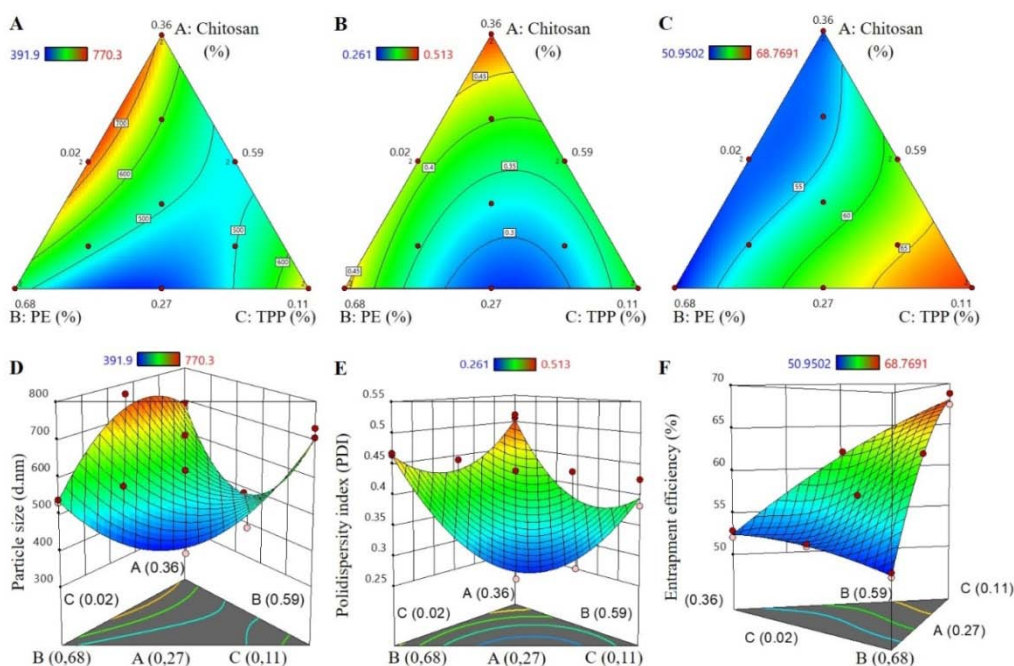


Fig. 2: Contour plot (A, B, and C) and 3D surface plot (D, E, and F)

The relationship between the dependent variable (Y₁) and the independent variable or factor (A, B, C) can be seen in the contour plot (fig. 2-A, 2-B, 2-C) and 3D surface plot (fig. 2-D, 2-E, 2-F). High chitosan concentrations tend to be obtained with larger particle sizes. However, low concentrations of chitosan do not always produce smaller particles. TPP in too low concentration tends to increase particle size diameter. Increased extract concentration will affect particle size but gives a more stable effect compared to chitosan and TPP. Chitosan at low concentrations can form smaller and more stable nanoparticles [30]. Adding a small amount of TPP with a large concentration of chitosan will cause the formation of micro-sized particles quickly. This is indicated by the presence of a suspension mist in solution.

Response of polydispersity index (Y₂)

The concentration of chitosan (A), ME (B), and TPP (C) can affect the increase in PDI from the resulting nanoparticle suspension. The highest PDI value (0.507) was generated in run 2. The experiment that was run 5 in SLD produced the lowest PDI, which was 0.261. Composition at run 2 and 5 (table 1) proves the effect of each component on the PDI obtained. Based on the contour plot (fig. 2-B) and 3D surface plot (fig. 2-E), the higher the concentration of chitosan will be obtained by the high PDI value. The high TPP concentration in its interaction with other components can reduce the PDI. Low PE concentrations in interaction with low chitosan

concentrations and high concentration TPP tend to decrease PDI. The most important characteristics in the nanoparticle system are the size and distribution of particles. Particle size distribution is expressed in the polydispersity index in the range between 0-1. Homogeneous dispersion is indicated by the PDI value close to 0, while PDI more than 0.5 indicates high heterogeneity.

Response of entrapment efficiency (Y₃)

Entrapment efficiency is an essential parameter in the development of material based on natural drug delivery systems [21, 23]. The percentage of entrapment efficiency can provide an overview of the effectiveness of active binding compounds by polymer complexes in the nanoparticle system. The model obtained for the absorption efficiency response (Y₃) is special quartic. The existence of an interaction variable of three ABC factors, with one quadratic component, becomes a special quartic with a square difference in the Y₁ and Y₂ responses.

Based on the regression equation (table 3), contour plot (fig. 2-C), and 3D surface plot (fig. 2-F), the interaction between the three components with a larger chitosan composition (A²BC) gives a decrease in the percentage of entrapment efficiency. The percentage of entrapment efficiency will increase in low concentration chitosan, low concentration extracts, and high concentration TPP. Experiments at run 1 and 9 (table 1) proved that the concentration

of extract and TPP greatly influenced the percentage of adsorption efficiency at constant chitosan concentrations.

Optimum formula and verification

Particle size and entrapment efficiency are the main parameters in the development of extract-based polyphenol compounds using this polymeric nanoparticle model. The priority value for both responses is given the highest. Absorption efficiency is given a maximum target in the hope that high active compounds (flavonoids) will be obtained. The model obtained from the SLD experiment was used to predict the optimum mixture composition. The optimum component mixture consisted of chitosan concentration as the primary polymer 0.270 %, ME 0.626 %, and TPP as the crosslinking agent 0.074 %.

The desirability value is used as an important indicator in determining the optimum mixture. The composition of the mixture with desirability value 0.841 will give a particle size diameter of 433.2 nm, a polydispersity index of 0.273 and a total flavonoid entrapment efficiency of 64.06 % (table 4). The intersection point of the optimal formula results can be seen in the contour plot (yellowish-orange area) with a desirability value 0.841 (fig. 3).

The particle size diameter in the optimum formula was 434.7 ± 3.90 nm, theoretically included in the 95 % range of verification CI (343.8-520.4 nm) and from 95 % range of PI (291.6-572, 5 nm) well verified. PDI and EE values were also well verified, in the range of 0.183 to 0.362 and 62.61 to 65.41 % (based on 95 % CI range).

Based on one sample t-test, particle size, PDI, and entrapment efficiency of the optimum formula there was no significant difference from the predictive value ($p > 0.05$).

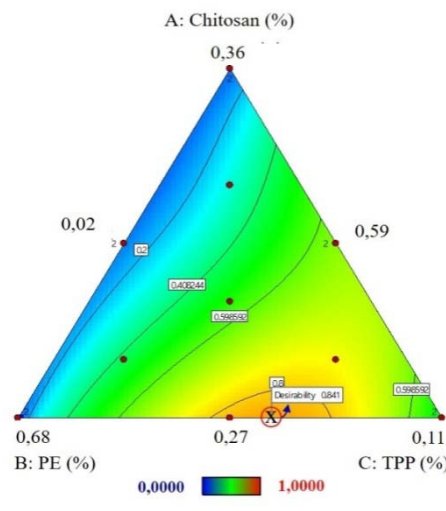


Fig. 3: Desirability

Table 4: Verification range from CI and PI

Response	Predicted	Observation*	95 % CI		95 % PI	
			Low	High	Low	High
Y ₁ : Particle size (d. nm)	432.1	434.7±3.90	343.8	520.4	291.6	572.5
Y ₂ : Polydispersity index (PDI)	0.273	0.285±0.03	0.183	0.362	0.130	0.415
Y ₃ : Entrapment efficiency (%)	64.01	62.98±0.40	62.61	65.41	61.99	66.03

*mean ($n=6$)±standard deviation (SD)

Zeta potential and electrophoretic mobility

In the nanoparticle formulation, high zeta potential is targeted because it relates to stability and effectiveness in drug delivery systems [31]. Small particles with high zeta potential represent high Brownian motion. Therefore, aggregation is not formed to increase stability in the dispersion system. When zeta potential is low, the attraction is greater than the repulsion force which causes dispersion to break, and particle flocculation occurs. The zeta potential value produced is 11.9 ± 0.1 mV with a positive charge. Although the zeta potential produced is relatively small, the nanoparticles are likely to be stabilized by the TPP layer through steric stabilization. Although zeta potential is only 20 mV or much lower but has steric stability, it can provide sufficient stabilization [32]. Steric stabilization involves the adsorption of polymers on the surface of the particles. Coatings adsorbed by polymers such as TPP will act as a barrier on the surface of the particles. That barrier will prevent particles from returning together because of the van der Waals attraction.

Electrophoretic mobility parameters, solids move in a liquid phase because there is an electric field applied to the system. As a result of this electric field, the particles will move, and their movement speed reaches the maximum when the electric force is proportional to the style of the friction. Electrophoresis phenomenon is characterized by electrophoretic mobility, which is the speed of unity of electric field strength ($\mu\text{mcm/Vs}$).

Characterization using FTIR-ATR

FTIR-ATR spectra are analyzed based on vibrations in the functional groups of each component material. The spectral patterns of the analysis results on chitosan, ME, TPP, and ME-NPs materials are shown in fig. 4. The spectra of the extract are strongly influenced by the specific and specific structure of the flavonoid and polyphenolic groups. Chitosan shows several typical peaks in the IR spectra, and

namely, absorption widened and overlap between stretching vibrations of O-H and N-H at wave numbers 3423 cm^{-1} . There is stretch vibration absorption C=O at wave number 1654 cm^{-1} and NH bending vibration at wave number 1596 cm^{-1} . The peak is a typical peak that marks the presence of amine and hydroxy groups in chitosan. There is also a stretching vibration of C-O-C from the glycoside bond at wave number 1079 cm^{-1} . The chitosan spectra of the measurement results are similar to some existing literature [33].

The extract used in this study is acidic with a pH of 4.83. The dominant polyphenol content causes the extract to be acidic. It also causes extracts to tend to be negatively charged. The ME spectra pattern (fig. 4-C) has a peak in the area of 3400 to 3200 cm^{-1} indicating the presence of an-OH group. The absorption peak at 2923 cm^{-1} marks the presence of a C-H group. The presence of aromatic C=C bonds is indicated by a vibration peak in the 1456 cm^{-1} area.

The interaction between components is estimated not only between chitosan and TPP. The positively charged group of chitosan can interact first with the negatively charged group of the extract. The interaction between constituent components is shown by the shift of several spectral peaks after being analyzed in the form of nanoparticles (fig. 4-D). The peak in the area of 3400 to 3200 cm^{-1} experienced a shift and widened. In addition to the new peak spectra, there is also a shift in the peak spectra of functional groups of each component. The peak of the spectra in the 1034 cm^{-1} area indicates the presence of P=O groups from TPP.

Morfologi using SEM

The morphological evaluation was carried out on the powder produced by drying the ME-NPs (lyophilized) using SEM. From the evaporation process, a gel-like texture with a thicker texture (gel aggregate) is obtained. This condition, caused by polyphenol compounds which dissolve in ethanol binds to chitosan so that the

interaction with acetic acid becomes weak and aggregate gel is formed when the solvent evaporation process. Gel aggregates will

become solid sheets with a drying process under high pressure. ME-NPs sheets obtained are then made into fine powder.

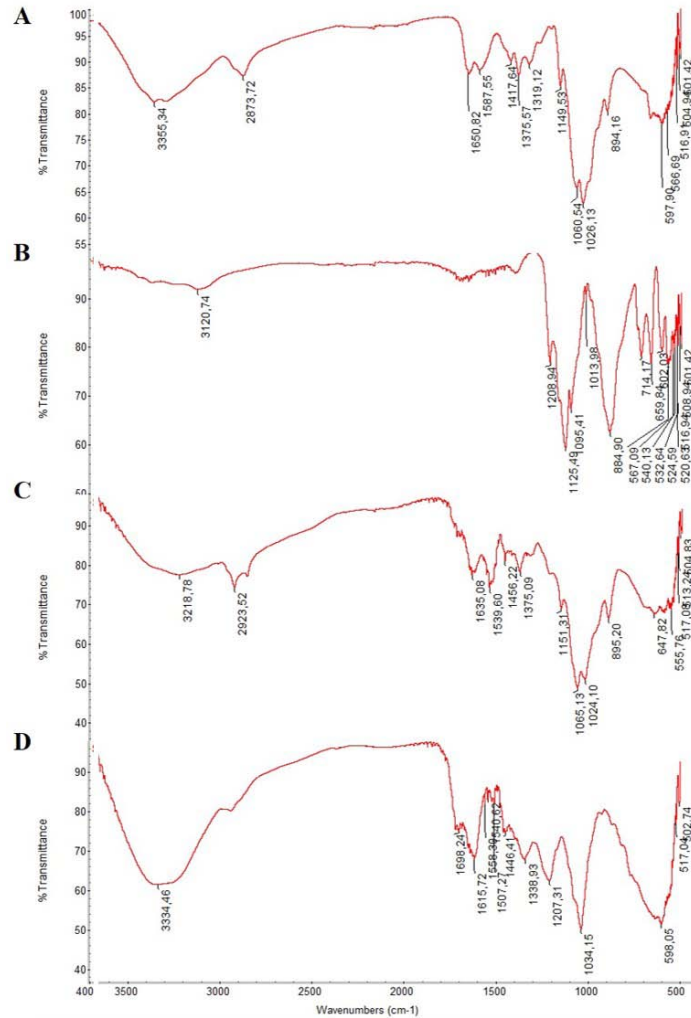


Fig. 4: FTIR-ATR spectra, chitosan (A), TPP (B), ME (C), and ME-NPs (D)

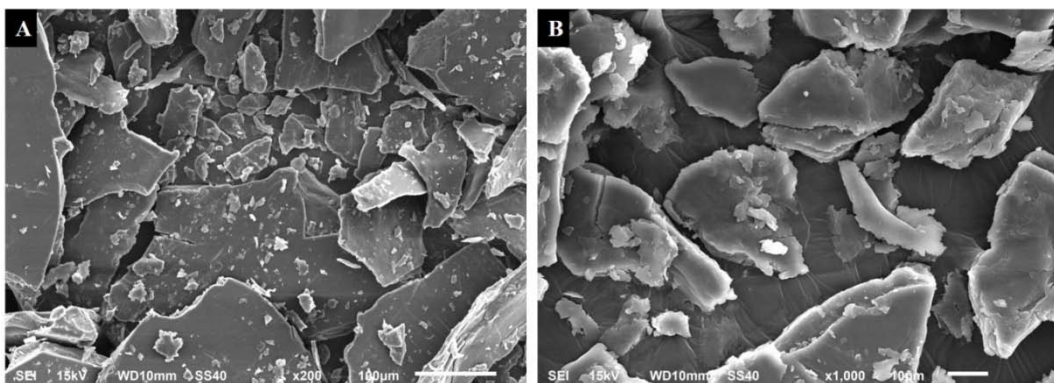


Fig. 5: Morphology of lyophilized powder particles from ME-NPs using SEM

Particle morphology of evaluation results with SEM is presented in the fig. 5. The particle morphology shown in the fig. is the layers that are stacked instead of spherical. Morphological conditions of spherical nanoparticles can be taken in liquid form (nanoparticle suspension). Therefore TEM instrumentation will be more precise in providing a general description. However, this study was not

conducted because ME-NPs powder material will be given to experimental animals in the immunomodulatory assay.

Nanoparticle stability assay

Stability is a condition that is good within certain limits throughout storage and uses or can be interpreted as the same characteristics as

when it was first made. The optimum formula was stored at room temperature and measured on days 1, 3, and 7. Physical stability was

observed from changes in particle size, PDI, and zeta potential values from the sample.

Table 5: Physical measurement of nanoparticles

Time (D)	Particle size* (d. nm)	Polydispersity index*	Zeta potential* (mV)	Electrophoretic mobility* ($\mu\text{cm}/\text{Vs}$)
1	428.9 \pm 17.9	0.307 \pm 0.021	11.9 \pm 0.1	0.933 \pm 0.007
3	402.0 \pm 2.4	0.276 \pm 0.003	12.1 \pm 0.8	0.947 \pm 0.058
7	393.2 \pm 9.2	0.256 \pm 0.012	13.4 \pm 0.6	1.050 \pm 0.044

*(n=3) mean \pm SD

Particle size has decreased on days 3 and 7 (table 5). The measured particles are probably particles that are still floating in the system. Small particles that combine to form agglomerates and tend to be unstable will form deposits at the bottom of the system and become undetectable at particle size measurements. The results of this study are following the theory of the effect of temperature on the size of chitosan nanoparticles which give results that at low-temperature storage of 10 to 25 °C the particle size is still relatively small [34]. Storage of chitosan nanoparticle solutions at temperature variations of -10, 5, and 25 °C. Temperature storage of -10 °C is ignored because of the stabilization of the nanoparticle solution. Significant particle size increases occurred at storage temperatures of 5 °C and 25 °C which were observed on days 15 and 7.

The PDI values observed on days 3 and 7 showed that nanoparticles still showed good homogeneity. Besides, the polydispersity index measured still meets the 95 % CI range of the values required by Design-Expert software. Electrophoretic mobility describes the speed of movement of charged particles in the system. The higher the value of electrophoretic mobility indicates that the faster the particles move. This causes the system to be more stable because there is no agglomeration. The ME-NPs is still stable on days 3 and 7 with storage conditions at room temperature.

Macrophage phagocytosis

Macrophage activity describes the percentage of active macrophage cells that can phagocytose latex (fig. 6). Visually from phagocytosis assay preparations, macrophage cells in ME-NPs appear to eat more of the latex granules (fig. 6-C). Phagocytosis index describes the ability of macrophage cells to be active in phagocytosis of latex (fig. 7-A). The phagocytic index is higher with the increasing number of phagocytic latex. ME-NPs treatment group had the highest phagocytosis index compared to other treatment groups. The water treatment group as a normal group had a phagocytosis index value of 1.43 \pm 0.07 and not much different from the CMC treatment group, which was 1.22 \pm 0.09.

The ME-NPs group showed the highest phagocytosis index compared to other groups, which were 3.04 \pm 0.15. The NPs-B (nanoparticles without extract) treatment group had a lower phagocytosis index value compared with ME-NPs, which was 1.61 \pm 0.09. Meniran herbal extracts that were not formulated had a phagocytosis index of 2.26 \pm 0.01. The results of the statistical

analysis of the phagocytosis index of macrophages showed that there were significant differences between ME-NPs groups with all treatment groups ($p < 0.05$).

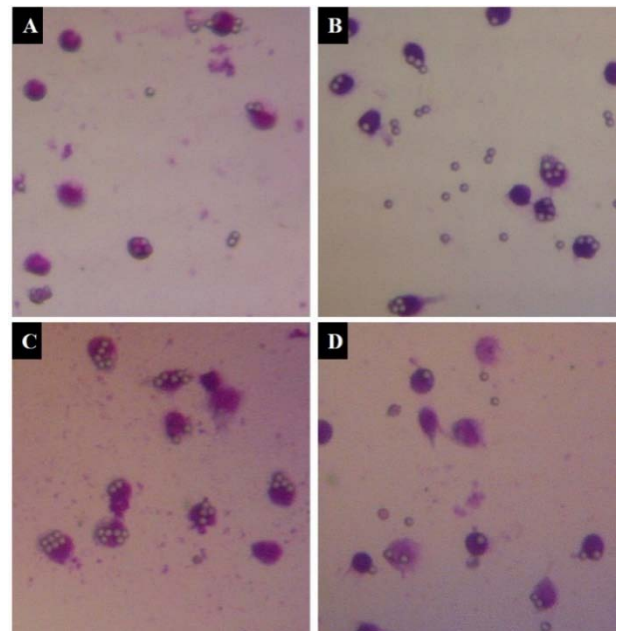


Fig. 6: Phagocytosis of macrophage cells, treatment with water (A), meniran extract (B), ME-NPs (C), and NPs-B (D)

The activity of macrophages in each treatment group is shown in fig. 7-B. ME-NPs showed macrophage phagocytosis activity of 89.00 \pm 3.61 % and unformulated extract (ME) of 79.89 \pm 0.93 %. Phagocytosis activity of ME-NPs also showed results that were significantly different from other groups ($p < 0.05$). The higher the percentage of macrophage cells that are active from a total of 100 macrophage cells counts, the more potential they will be as immunostimulants [27].

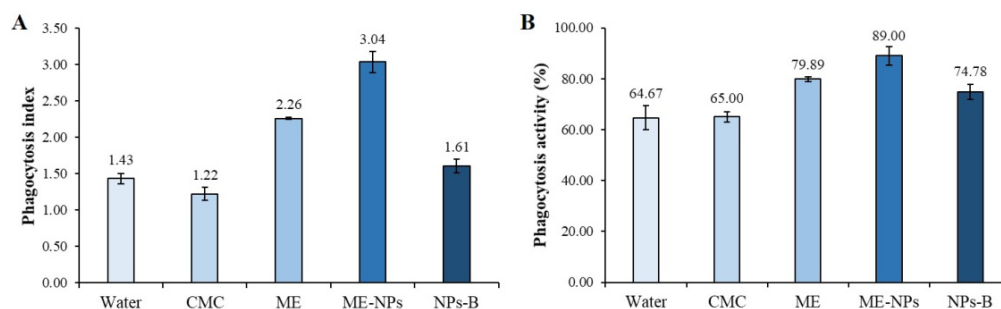


Fig. 7: Phagocytosis index (A) and phagocytosis activity (B) (n=6)

Nitric oxide (NO)

Macrophages can destroy antigens by respiratory burst and produce ROS such as superoxide, hydrogen peroxidase and nitric oxide (NO). Nitric oxide is a powerful microbicidal agent against intracellular microorganisms. Nitric oxide is a parameter that shows the activation of macrophage cells [4,10]. Nitric oxide was measured from the supernatant culture of peritoneal macrophages (fig. 8).

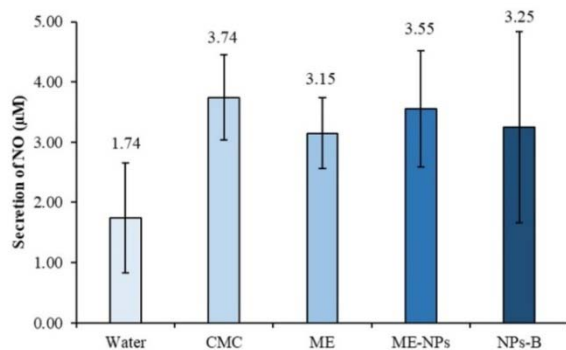


Fig. 8: NO secretion from each treatment group (n=6)

ME-NPs were not significantly different from extract ($p>0.05$) but were significantly different from NPs-B ($p<0.05$). Improved macrophage performance is accompanied by increased phagocytosis. Active phagocytes (macrophages and neutrophils) will secrete NO. Nitric oxide can attack the cells that produce it and the cells that surround it to enable a decrease in NO levels despite high activity [10].

Immunomodulatory activity

Meniran herbal extract formulated in the form of polymeric nanoparticles has a higher immunomodulatory activity than unformulated extract. The stability of active substances reaching the systemic circulation becomes an essential factor in increasing the activity of immunomodulators. Also, optimal activity is influenced by the absorption and release of active substances into the systemic circulation. Flavonoids have low water solubility even in the form of glycosides. Flavonoids have low bioavailability and are easily modified due to environmental factors such as temperature, pH, and light. The mechanism of the absorption of flavonoids in the gastrointestinal causes a small number of flavonoids absorbed in the small intestine [35]. Flavonoids can be modified into other forms before reaching the absorption area due to degradation by microorganisms or enzymes in the intestine [36].

Nano-sized drug delivery systems significantly affect the absorption profile of active substances. Polymeric nanoparticles can increase solubility, bioavailability, efficacy, reduce doses, and increase absorption of herbal medicines [37]. Particle size, morphology, and character of the surface play an important role in absorption through the gastrointestinal mucosa [35]. The surface area becomes larger as the particle size decreases so that most of the drug will be near the surface of the particle. In these conditions, drug release becomes faster. Larger particles have larger nuclei so more drugs can be packaged and diffuse slowly [38].

Some publications formulate polyphenol compounds, especially quercetin in the form of nanoparticles. Chitosan nanoparticles are formulated to improve the oral bioavailability of flavonoids [35]. The antioxidant activity of quercetin can be increased in the chitosan-alginate nanoparticle formula [39]. Polymer nanoparticles with routine active substances have been formulated using chitosan and TPP in the form of nanoparticles [40]. Nanoparticle formula using chitosan was detected stably in gastric fluid media, while the stability in simulated intestinal fluid media was only 20 % released and 80 % was still absorbed in chitosan nanoparticles. Positively charged nanoparticles are absorbed through mucoadhesive, polymeric nanoparticles tend to show high levels

of drug release. This is very important in the oral administration route to ensure that no drug is released from preparation before reaching the systemic circulation [35].

Administration of ME-NPs has been shown to increase phagocytic index and phagocytic activity. Chitosan as the primary polymer in the formula gives different results compared to other test groups. Mechanisms related to the effectiveness of ME-NPs as immunomodulators still need to be studied further regarding drug delivery and other immunological activity parameters. Based on the theory, the positive charge of polymer particles helps to interact with the intestinal mucous membrane which helps in the release and absorption of active compounds.

Chitosan has been proven *in vitro* and *in vivo* to increase drug absorption due to the mucoadhesive ability and tight junction opening in mucous cell membranes [17, 41]. The interaction of chitosan which is positively charged and the negative charge of mucin causes a long contact time between the drug and the absorption surface. This condition causes an increase in drug absorption. Chitosan nanoparticles have unique features in absorption, namely by M cells and follicles in lymphoid tissues that are connected to the intestine in the gastrointestinal system. After reaching the apical membrane of intestinal epithelial cells, most of the nanoparticles cross the enterocytes through transcellular transport. Nanoparticles enter the bloodstream or lymphatic vessels through exocytosis. Particles measuring less than 500 nm enter through endocytosis with mediators clathrin and caveolae. The ion or cationic layer of chitosan protects polymeric nanoparticles from endolysosomal degradation in enterocytes [35, 41].

CONCLUSION

Meniran herbal ethanolic extract was successfully formulated into polymeric nanoparticles using chitosan-tripolyphosphate. Extracts in the nanoparticle formula produced a higher phagocytic index value and phagocytic activity of macrophages which was better than the unformulated extract. Evaluation of other parameters of immunomodulatory activity is needed to produce superior starting material as nano-herbal development.

ACKNOWLEDGMENT

The authors gratefully acknowledge the financial support by Grants 2017 (Hibah Pengembangan Penelitian Laboratorium) No. UGM/FA/1677a/M/05/01, Faculty of Pharmacy, Universitas Gadjah Mada, Yogyakarta. Thanks to PT. DKSH Indonesia who have co-sponsored this research.

AUTHORS CONTRIBUTIONS

The authors declare that this work was performed by all authors named in this article, and all liabilities pertaining to claims relating to the content of this article will be borne by all of them. All authors approved and read the manuscript for publication.

CONFLICT OF INTERESTS

The authors declare that no conflict of interest is associated with this work

REFERENCES

1. Tjandrawinata RR, Susanto LW, Nofiarny D. The use of *Phyllanthus niruri* L. as an immunomodulator for the treatment of infectious diseases in clinical settings. *Asian Pac J Trop Dis* 2017;7:132-40.
2. Nworu CS, Akah PA, Okoye FBC, Esimone CO. Aqueous extract of *Phyllanthus niruri* (Euphorbiaceae) enhances the phenotypic and functional maturation of bone marrow-derived dendritic cells and their antigen-presentation function. *Immunopharmacol Immunotoxicol* 2010;32:393-401.
3. Nworu CS, Akah PA, Okoye FBC, Proksch P, Esimone CO. The effects of *Phyllanthus niruri* aqueous extract on the activation of murine lymphocytes and bone marrow-derived macrophages. *Immunol Invest* 2010;39:245-67.
4. Kumar S, Sharma S, Kumar D, Kumar K, Arya R. Immunostimulant activity of *Phyllanthus reticulatus* poir: a

- useful plant for infectious tropical diseases. Asian Pac J Trop Dis 2014;4:S491-5.
5. Shiyan S, Herlina H, Rizkika Sari L. Nephroprotective of anthocyanin pigments extract from red cabbage (*Brassica oleracea* L. Var. Capitata f. Rubra) against gentamicin-captopril-induced nephrotoxicity in rats. Asian J Pharm Clin Res 2018;11:432-6.
 6. Shiyan S, Herlina H, Bella M, Amriani A. Antiobesity and anti-hypercholesterolemic effects of white tea (*Camellia sinensis*) infusion on high-fat diet induced obese rats. Pharmacia 2017;7:278-88.
 7. Mustarichie R, Priambodo D. Tablet formulation from meniran (*Phyllanthus niruri* L.) extract with a direct compression method. Int J Appl Pharm 2018;10:98-102.
 8. Ilangkovan M, Jantan I, Mesaik MA, Bukhari SNA. Immunosuppressive effects of the standardized extract of *Phyllanthus amarus* on cellular immune responses in wistar-kyoto rats. Drug Des Devel Ther 2015;9:4917-30.
 9. Afolayan FID, Erinwusi B, Oyeyemi OT. Immunomodulatory activity of curcumin-entrapped poly d,l-lactic-co-glycolic acid nanoparticles in mice. Integr Med Res 2018;7:168-75.
 10. Putri DU, Rintiswati N, Soesatyo MH, Haryana SM. Immune modulation properties of herbal plant leaves: *Phyllanthus niruri* aqueous extract on immune cells of tuberculosis patient-*in vitro* study. Nat Prod Res 2018;32:463-7.
 11. Kumari A, Yadav SK, Pakade YB, Singh B, Yadav SC. Development of biodegradable nanoparticles for delivery of quercetin. Colloids Surf B 2010;80:184-92.
 12. Kumari DR, Kotecha DM. A review on the standardization of herbal medicines. Int J Pharma Sci Res 2016;7:10.
 13. Rasheed A, Reddy SB, Roja C. A review on standardization of herbal formulation. Int J Phytother 2012;2:74-88.
 14. Wang W, Sun C, Mao L, Ma P, Liu F, Yang J, et al. The biological activities, chemical stability, metabolism and delivery systems of quercetin: a review. Trends Food Sci Technol 2016;56:21-38.
 15. Saikia C, Gogoi P, Maji TK. Chitosan: a promising biopolymer in drug delivery applications. J Mol Genet Med 2015;S4:1-10.
 16. Azuma K, Izumi R, Osaki T, Ifuku S, Morimoto M, Saimoto H, et al. Chitin, chitosan, and its derivatives for wound healing: old and new materials. J Funct Biomater 2015;6:104-42.
 17. Nagpal K, Singh SK, Mishra DN. Chitosan nanoparticles: a promising system in novel drug delivery. Chem Pharm Bull 2010;58:1423-30.
 18. Sawtarie N, Cai Y, Lapitsky Y. Preparation of chitosan/tripolyphosphate nanoparticles with highly tunable size and low polydispersity. Colloids Surf B 2017;157:110-7.
 19. Sreekumar S, Goycoolea FM, Moerschbacher BM, Rivera-Rodriguez GR. Parameters influencing the size of chitosan-TPP nano- and microparticles. Sci Rep 2018;8:1-11.
 20. Al-Nemrawi NK, Alsharif SSM, Dave RH. Preparation of chitosan-TPP nanoparticles: the influence of chitosan polymeric properties and formulation variables. Int J Appl Pharm 2018;10:60-5.
 21. Anju K, Jegadeeshwari AL, Gandhi NN. Optimization of green synthesized silver nanoparticles from *Caralluma umbellata*. Int J Appl Pharm 2018;10:103-10.
 22. Martien R, Loretz B, Schnürch AB. Oral gene delivery: design of polymeric carrier systems shielding toward intestinal enzymatic attack. Biopolymers 2006;83:327-36.
 23. Chabib L, Martien R, Ismail H. Formulation of nanocurcumin using low viscosity chitosan polymer and its cellular uptake study into T47D cells. Indones J Pharm 2012;23:27-35.
 24. Hirlekar SDS, Bhairy S, Bhairy S, Hirlekar R, Hirlekar R. Preparation and characterization of oral nanosuspension loaded with curcumin. Int J Pharm Pharm Sci 2018;10:90-5.
 25. Chang CC, Yang MH, Wen HM, Chern JC. Estimation of total flavonoid content in propolis by two complimentary colorimetric methods. J Food Drug Anal 2002;10:178-82.
 26. Shiyan S, Hertiani T, Martien R, Nugroho AK. Optimization of a novel kinetic-assisted infundation for rich-EGCG and polyphenols of white tea (*Camellia sinensis*) using central composite design. Int J Appl Pharm 2018;10:259-67.
 27. Nurrochmad A, Ikawati M, Sari IP, Murwanti R, Nugroho AE. Immunomodulatory effects of ethanolic extract of *Thyphonium flagelliforme* (Lodd) Blume in rats induced by cyclophosphamide. J Evid-Based Complement Altern Med 2015;20:167-72.
 28. Kulig D, Zimoch Korzycka A, Król Ż, Oziembłowski M, Jarmoluk A, Kulig D, et al. Effect of film-forming alginate/chitosan polyelectrolyte complex on the storage quality of pork. Molecules 2017;22:98.
 29. Venkatesan J, Bhatnagar I, Kim SK. Chitosan-alginate biocomposite containing fucoidan for bone tissue engineering. Mar Drugs 2014;12:300-16.
 30. Tsai ML, Chen RH, Bai SW, Chen WY. Storage stability of chitosan/tripolyphosphate nanoparticles in a phosphate buffer. Carbohydr Polym 2011;84:756-61.
 31. Parmar N, Singla N, Amin S, Kohli K. Study of cosurfactant effect on nanoemulsifying area and development of lercanidipine loaded (SNEDDS) self nanoemulsifying drug delivery system. Colloids Surf B 2011;86:327-38.
 32. Honary S, Zahir F. Effect of zeta potential on the properties of nano-drug delivery systems—a review (Part 2). Trop J Pharm Res 2013;12:265-73.
 33. Mukhopadhyay P, Chakraborty S, Bhattacharya S, Mishra R, Kundu PP. pH-sensitive chitosan/alginate core-shell nanoparticles for efficient and safe oral insulin delivery. Int J Biol Macromol 2015;72:640-8.
 34. Fan W, Yan W, Xu Z, Ni H. Formation mechanism of monodisperse, low molecular weight chitosan nanoparticles by ionic gelation technique. Colloids Surf B 2012;90:21-7.
 35. Bilia AR, Isacchi B, Righeschi C, Guccione C, Bergonzi MC. Flavonoids loaded in nanocarriers: an opportunity to increase oral bioavailability and bioefficacy. Food Nutr Sci 2014;05:1212-327.
 36. Williamson G, Manach C. Bioavailability and bioefficacy of polyphenols in humans. II. Review of 93 intervention studies. Am J Clin Nutr 2005;81:243S-255S.
 37. Thapa RK, Khan GM, Parajuli-Baral K, Thapa P. Herbal medicine incorporated nanoparticles: advancements in herbal treatment. Asian J Biomed Pharm Sci 2013;3:7-14.
 38. Redhead HM, Davis SS, Illum L. Drug delivery in poly(lactide-co-glycolide) nanoparticles surface modified with poloxamer 407 and poloxamine 908: *in vitro* characterisation and *in vivo* evaluation. J Controlled Release 2001;70:353-63.
 39. Aluani D, Tzankova V, Kondeva Burdina M, Yordanov Y, Nikolova E, Odzhakov F, et al. Evaluation of biocompatibility and antioxidant efficiency of chitosan-alginate nanoparticles loaded with quercetin. Int J Biol Macromol 2017;103:771-82.
 40. Konecsni K, Low NH, Nickerson MT. Chitosan-tripolyphosphate submicron particles as the carrier of entrapped rutin. Food Chem 2012;134:1775-9.
 41. Mohammed MA, Syeda JTM, Wasan KM, Wasan EK. An overview of chitosan nanoparticles and its application in non-parenteral drug delivery. Pharmaceutics 2017;9:53-79.